International Forum on Aeroelasticity and Structural Dynamics
IFASD 2019
9-13 June 2019, Savannah, Georgia, USA

COUPLING OF AEROELASTIC AND PILOT DYNAMICS VIA BIODYNAMIC-FEEDTHROUGH IN PILOT-AUGMENTED OSCILLATIONS

Daniel Drewiacki[1], Flávio J. Silvestre[2], Antônio Bernardo Guimarães Neto[3]

[1]Instituto Tecnológico de Aeronáutica
São José dos Campos, SP, Brazil
daniel.drewiacki@gmail.com

[2]Technische Universitat Berlin
Berlin, Germany
flavio.silvestre@tu-berlin.de

[3]Instituto Tecnológico de Aeronáutica
São José dos Campos, SP, Brazil
antonio@ita.br

Keywords: aeroservoelasticity, biodynamic feedthrough, pilot-augmented oscillations

Abstract: Biodynamic feedthrough is a phenomenon in which structural vibrations on the cockpit are fedback to the pilot, who transmits those vibrations on the aircraft through involuntary inceptor displacements. In the case these commands lead to instabilities, the phenomenon is then called Pilot-Assisted (or Augmented) Oscillations (PAO). This is a complex phenomenon that depends on three basic elements. First element is the aeroelastic modes of the aircraft, especially their modal shapes (since only specific modal shapes interfere in this phenomenon) and frequencies. Second one is the inceptor's system characteristics, such as natural frequency and damping. The last element is the human pilot dynamics, which may be modelled as a passive spring-mass-damper system. This paper aims to explore how these three elements affect the development of the PAO phenomenon for more flexible aircraft. The investigations herein are accomplished for a virtual, flexible aircraft by the analysis of pilot-in-the-loop simulations of a high gain maneuver, varying airframe elasticity levels, inceptor system parameters and pilot model characteristics.

1 INTRODUCTION

Since the beginning of powered flight there always was a major concern on airframe efficiency. In the last past decades, this concern has led to the development of more elastic aircraft, which means that the frequency range of the elastic-body dynamics is getting closer to the rigid-body dynamics. This approximation may potentialize issues such as the biodynamic feedthrough, a phenomenon in which the structural vibrations on the cockpit are fedback to the pilot, that acts as a passive agent and transmits high-frequency, involuntary commands, to the inceptors (yoke, centerstick or sidestick). If instabilities develop and the occurrence of limit-cycle or divergent oscillations are noticed, the phenomenon is then called Pilot-Augmented Oscillations (PAO). Even though PAO is caused due to an anomalous interaction between the pilot and the airframe, this phenomenon is quite different from the PIO (Pilot-Induced Oscillations) phenomenon, since the pilot is an active agent in the latter.

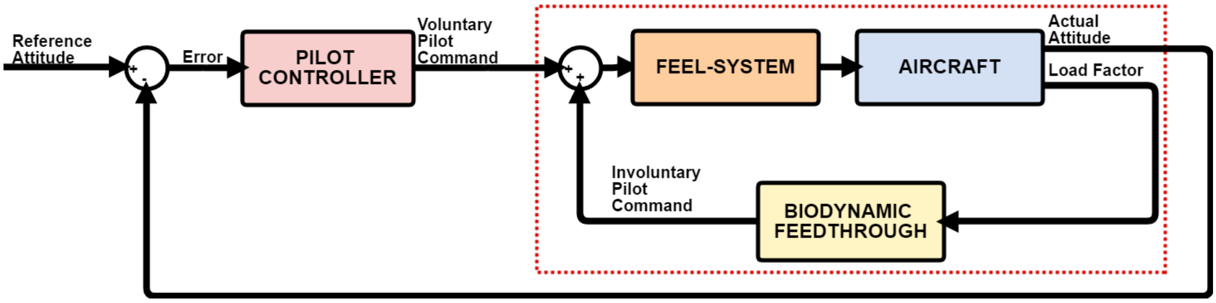

Figure 1: Pilot-vehicle system represented with inclusion of a Biodynamic Feedthrough model.

Mainly due to the frequency range of the elastic modes, PAO is a phenomenon that is more common on rotary-wing aircraft, as noted by Walden [1] and Muscarello [2]. However, as noted by Allen [3], it may happen on fixed-wing aircraft as well, especially those equipped with sidestick controllers as the feel-system type. Nevertheless, Lee and Vining [4] presented a PAO occurrence that happened in an aircraft with the yoke as inceptor type.

In order to better understand this phenomenon and the role of the human pilot, Allen [3] presented an interesting study by modelling the involuntary part of the pilot command as a spring-mass-damper system. Tests were made in a fixed base simulator with a platform vibrating according to the aircraft model to simulate structural vibration. Pilots with different statures and weights were asked to perform synthetic tracking tasks using a sidestick. The author was able then to extract a transfer function from cockpit accelerations to involuntary pilot stick displacements.

Figure 1 represents the pilot-vehicle system adopted in this paper with the inclusion of a mixed pilot model and also a model for the feel-system dynamics. Previous research published by Drewiacki et al [5] proposed the adoption of this mixed pilot model, comprising both voluntary and involuntary inceptor commands. The compensatory pilot model proposed by McRuer [7] was adopted for the voluntary part, while the biodynamic feedthrough model proposed by Allen [3] was considered for the involuntary commands.

Regarding the feel-system model, the inceptor dynamics is in a frequency range that does not affect the rigid body modes of the aircraft, and therefore is neglected or simplified in many handling qualities studies. But this dynamics can affect and also be affected by the lower frequency flexible body modes. For this reason, this model is included in the analysis presented in this paper.

Even though PAO is even more rare than PIO, the increasing elasticity of airframe structure may lead to a potential growth in the number of occurrences of this phenomenon. In fact, PAO can be avoided by considering the inclusion of notch filters to decouple rigid-body and elastic-body dynamics. However, as demonstrated by Drewiacki et al [5], the cost of the introduction of such device is an increase in delays that can be prohibitive and lead to the PIO-proneness of the aircraft. Another simple and cheap, but limited solution, is to provide an armrest for the pilot, as studied by Venrooij et al [6].

So far there are no established criteria for the prediction and prevention of the PAO problem as there are for the PIO problem. In order to allow the future development of such criteria, this paper proposes to investigate the occurrences of PAO by varying characteristics of the blocks presented in Fig. 1. Airframe flexibility is evaluated in different levels, corresponding to variations on the flexible modes frequencies. Inceptor model parameters such as natural frequency and damping effects are also evaluated. For what concerns pilot models, the voluntary pilot commands model is considered fixed, as the cognitive commands are in a low frequency range and do not affect the occurrences of PAO. On the other hand, variability in the biodynamic feedthrough model, directly responsible for PAO, is studied.

2 SIMULATION MODELS

2.1 Aircraft Model

In this paper we consider the GNBA model proposed by Guimarães Neto [8]. This model was defined in the state-space form, considering the six-degree-of-freedom aircraft motion and the elastic modes with amplitudes η_i and with frequencies up to 25 Hz. Elastic body dynamics model consider the methodology proposed by Waszak and Schmidt [11], which introduces two dynamic states for each vibration mode that are represented by η_i and $\dot{\eta_i}$. The flexible model used in this paper has, in addition, a set of aerodynamic lag states represented by λ that model the effects of the flow unsteadiness modeled with the doublet-lattice method (developed by Albano and Rodden [9]) and approximated by rational functions as per Eversman and Tewari [10] and Guimarães Neto [8].

$$\begin{aligned} \dot{x} &= Ax + Bu \\ y &= Cx + Du \end{aligned} \tag{1}$$

$$x = \left[\begin{array}{ccccccccccccccc} V & \alpha & q & \theta & H & X_{dist} & \beta & \phi & p & r & \psi & Y_{dist} & \eta_i & \dot{\eta_i} & \lambda \end{array} \right]^T \tag{2}$$

$$u = \left[\begin{array}{ccccc} i_H & \delta_{elev} & \delta_{ail} & \delta_{rud} & \delta_{throttle} \end{array} \right]^T \tag{3}$$

In all the analysis presented in this paper, three different elasticity levels of the GNBA are considered. First level is the Nominal flexibility level. Second one is called W050F050 due to both wing and fuselage stiffness reduced to 50% of the Nominal value. Similarly, third level is called W025F025. A fourth level, corresponding to a purely Rigid Body model, is considered only as a reference for the analysis. Table 1 below shows the natural frequencies of the GNBA models.

Table 1: Natural frequencies of simulation models in [rad/s]

Natural Mode	Rigid Body	Nominal	W050F050	W025F025
Phugoid	0.109	0.105	0.107	0.104
Short Period	1.68	1.58	1.55	1.47
Dutch Roll	1.54	1.50	1.49	1.46
Spiral	0.018	0.020	0.022	0.026
Roll	1.97	1.80	1.76	1.56
η_1	-	15.2	12.3	11.1
η_2	-	19.7	15.2	12.5
η_3	-	23.3	19.6	14.1
η_4	-	24.5	20.5	14.8
η_5	-	27.8	22.7	19.2
η_6	-	28.4	23.4	20.2
η_7	-	34.5	27.6	21.9
η_8	-	36.4	30.2	22.7

2.2 Pilot models

The pilot model adopted in this work is a mixed model that comprises both voluntary and involuntary pilot commands, as shown in Fig. 1.

The block labeled as Pilot Controller corresponds to the compensatory pilot modeled by the transfer function of Eq. (4), considering as input the error $E(s)$ to be minimized and as output the amount of control inceptor displacement δ_{stick} necessary. The transfer function is composed of a gain K_{pilot}, an effective time delay $e^{-\tau_h s}$ and a zero-pole pair corresponding to the terms $(T_{Lead}s + 1)$ and $(T_{Lag}s + 1)$, which is an anticipation or posticipation factor used by the pilot in order to compensate for aircraft's natural response. For this present study, the parameters of this model were kept fixed. It was set K_{pilot} = 1, τ_h = 0.3, and it was considered only the anticipation factor as T_{Lead} = 0.5 and T_{Lag} = 0.

$$Y_{pilot}(s) = \frac{\delta_{stick}}{E(s)} = K_{pilot}e^{-\tau_h s}\frac{(T_{Lead}s + 1)}{(T_{Lag}s + 1)} \quad (4)$$

The undesirable effect of involuntary commands can be studied by including the block labeled as Biodynamic Feedthrough in Fig. 1. This block corresponds to the passive pilot dynamics that introduces involuntary stick commands due to structural vibration.

Equation 5 shows the baseline transfer function. According to the study presented by Coermann [12], this transfer function corresponds to the pilot in the sitting relaxed position. Eqs. 6 and 7 show the transfer functions for the sitting erect and standing erect positions respectively.

$$G_{BDFT_1}(s) = \frac{\delta_{stick}}{n_z} = \frac{2260}{s^2 + 22.62s + 1560} \quad (5)$$

$$G_{BDFT_2}(s) = \frac{\delta_{stick}}{n_z} = \frac{3293}{s^2 + 34.26s + 1663} \quad (6)$$

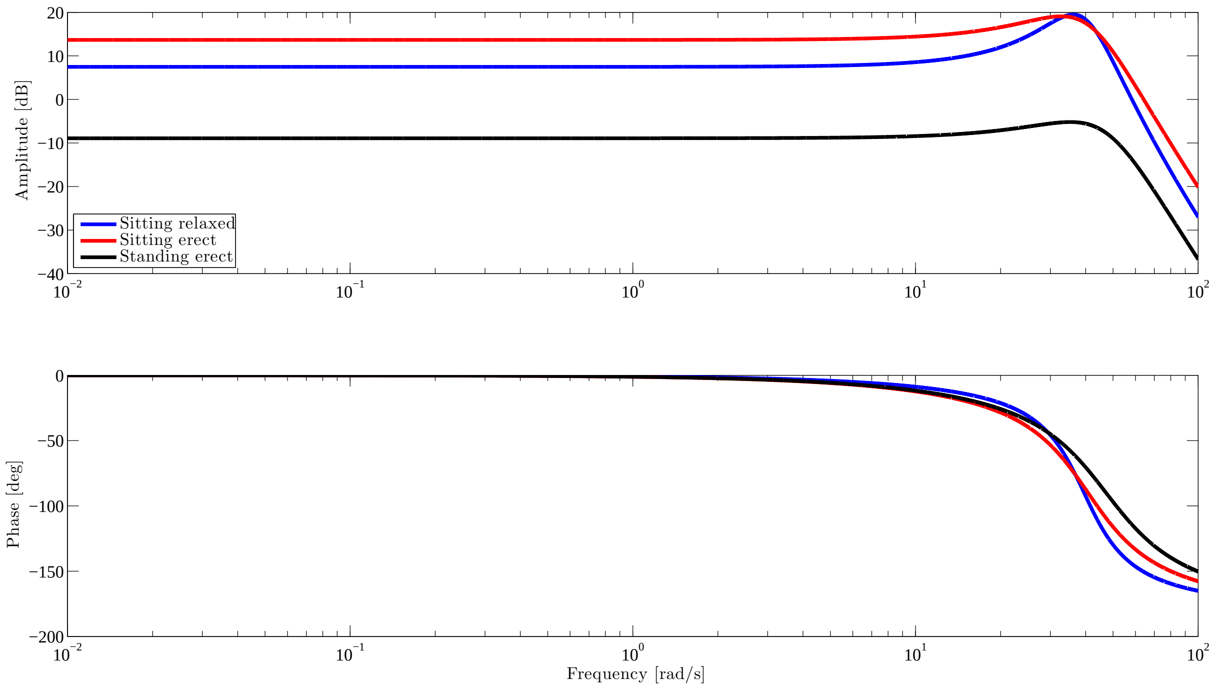

Figure 2: Bode plots for the different biodynamic feedtrough transfer functions.

$$G_{BDFT_3}(s) = \frac{\delta_{stick}}{n_z} = \frac{1428}{s^2 + 44.42s + 2231} \tag{7}$$

The Bode plots corresponding to these transfer functions can be seen in Fig. 2. Notice that transfer function corresponding to the sitting erect position presents a higher gain at low frequencies, while transfer function corresponding to the standing erect position presents attenuation in the whole frequency range. The resonant peak near 6 Hz has almost the same magnitude for both sitting relaxed and erect positions.

2.3 Inceptor Model

Even though there are some cases of PAO related with yoke dynamics, the involuntary pilot model for biodynamic feedthrough adopted in this paper was developed for aircraft equipped with the sidestick as the feel-system. A formulation of a biodynamic feedthrough pilot model for aircraft equipped with the yoke or the centerstick would require adjustments, as ergonomics influence the interaction between the pilot and the feel-system.

The sidestick dynamics is modelled as a second-order system as shown in Eq. 8. The parameters for both the feel-system damping ξ_{stick} and natural frequency $\omega_{n_{stick}}$ will be varied (representing parameters of real systems) in order to evaluate how they can affect the occurrences of PAO.

$$G_{stick}(s) = \frac{\omega_{n_{stick}}^2}{s^2 + 2\xi_{stick}\omega_{n_{stick}}s + \omega_{n_{stick}}^2} \tag{8}$$

3 RESULTS

In this section there will be presented the results of pilot-in-the-loop simulations performed considering a gross acquisition pitch capture maneuver of 5^o of amplitude. This maneuver is

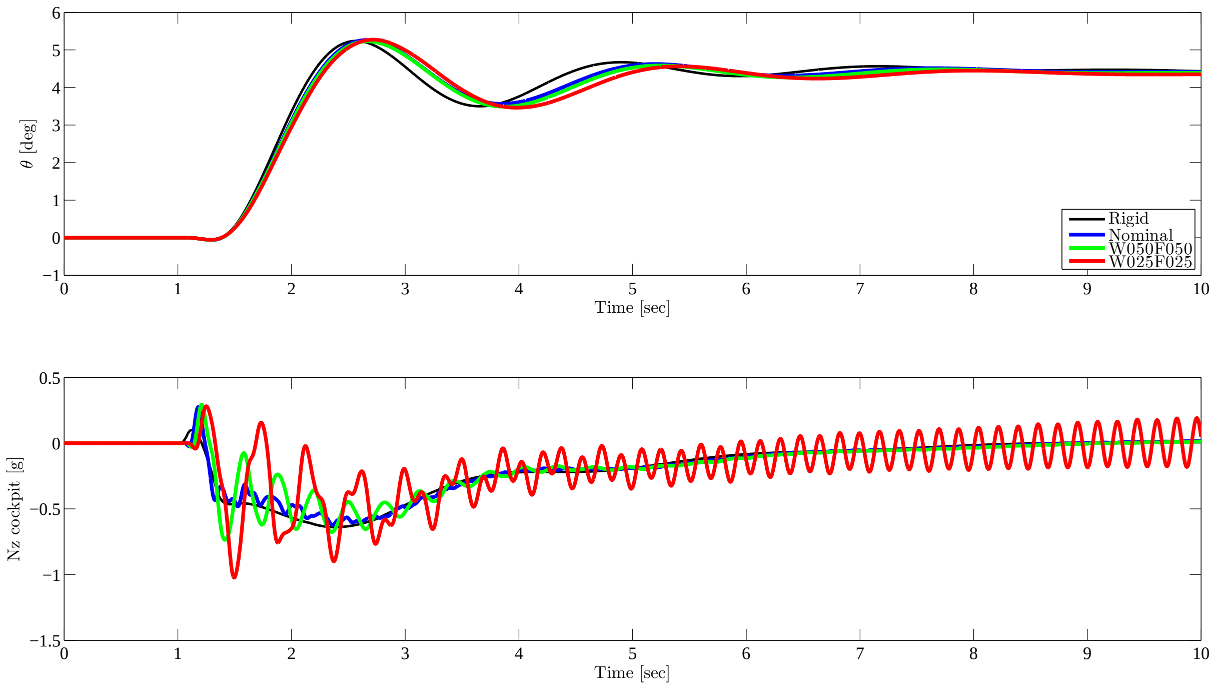

Figure 3: Pitch capture simulation for the sitting relaxed position.

described in guidance AC 25-7C [13] as part of a flight test campaign to explore PIO. Even though PIO and PAO are different phenomena, since they are not related to the same root-causes, the intention of this maneuver is to assess the aircraft response characteristics in a high-frequency range.

In the first part of this section there will be presented the effects of variations on the biodynamic feedthrough model for the PAO occurrences. Feel-system dynamics is neglected in this first part, and the transfer function is set to a unity gain. In the second part, the effects due to inceptor dynamics variations are analyzed, and the biodynamic feedthrough effect is kept fixed in a reference baseline. In all the simulations presented, the effects of increasing airframe elasticity are evaluated. On the other hand, the voluntary pilot model is kept unchanged for all the simulations considered.

3.1 Involuntary pilot model effects

In the first simulation, it is considered the biodynamic feedthrough model corresponding to the sitting relaxed position. Figure 3 shows the main results for the pitch capture maneuver simulation, which are the pitch angle measured at the CG (the target for this maneuver) and the load factor measured in the cockpit, which is the input variable of the biodynamic feedthrough model.

Figure 4 shows both the voluntary and involuntary pilot commands during the execution of this maneuver. It can be concluded that the high frequency oscillation observed in the load factor measured in the cockpit is related to the involuntary pilot commands, as both oscillations occur in the same frequency, of around 36 rad/s. This frequency corresponds to the second vertical fuselage bending mode. In fact, this is a closed-loop instability in the inner loop of the PVS model presented in Fig. 1. In other words, this is an example of a Pilot-Augmented Oscillation, or PAO.

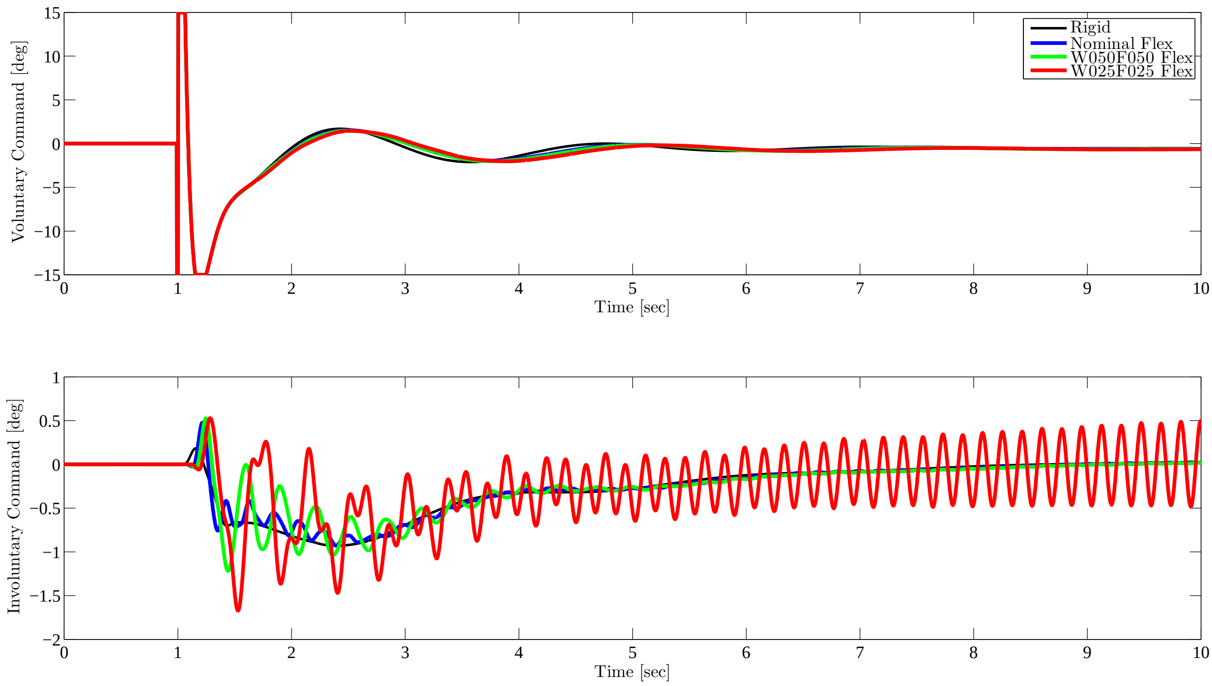

Figure 4: Pilot commands for the sitting relaxed position.

Figures 5 and 6 show the results for the gross acquisition capture task for the sitting erect position. It can be seen that very similar results are achieved with transfer function corresponding to the sitting relaxed position that were shown in Figs. 3 and 4.

Overall values of load factor are smaller in the sitting erect position when compared to the sitting relaxed position. Also, the amplitude of the high frequency oscillation corresponding to the PAO is smaller in the sitting erect position. This result can be explained as the sitting erect position transfer function has a higher magnitude in all frequency range. Therefore, the amplitudes of the involuntary commands will be higher when compared to the sitting relaxed position. When voluntary and involuntary commands are in contrast, the final result is a smaller control inceptor displacement, reducing the command sensitivity.

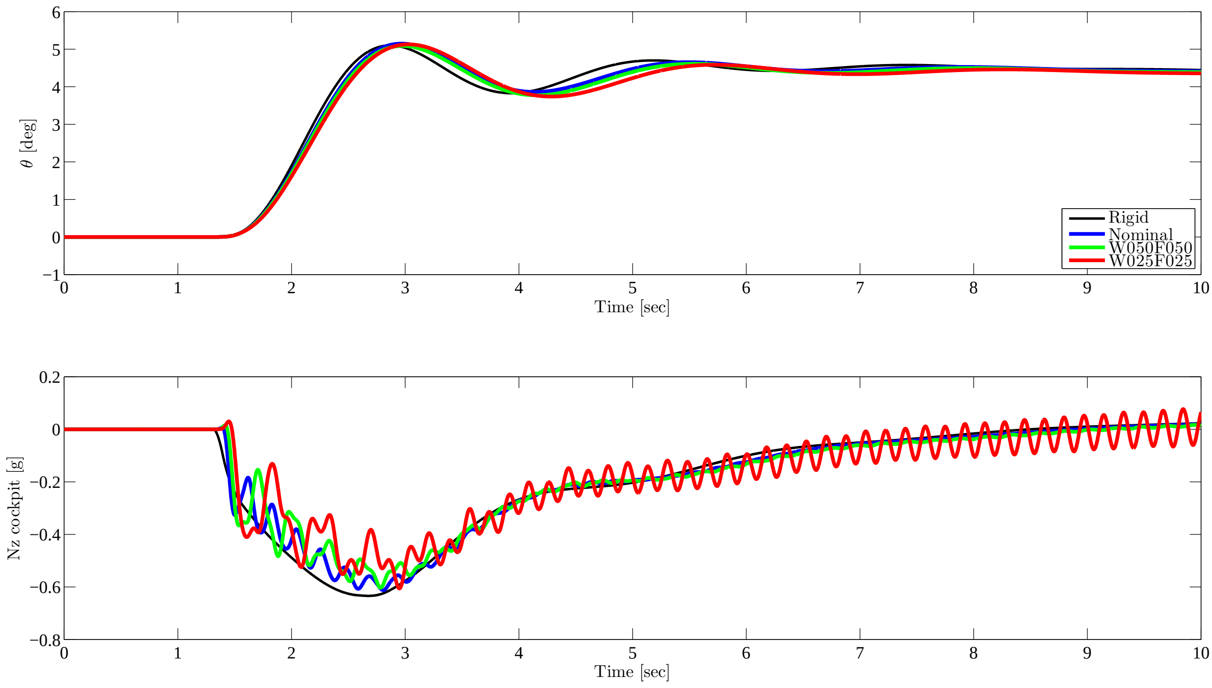

Figure 5: Pitch capture simulation for the sitting erect position.

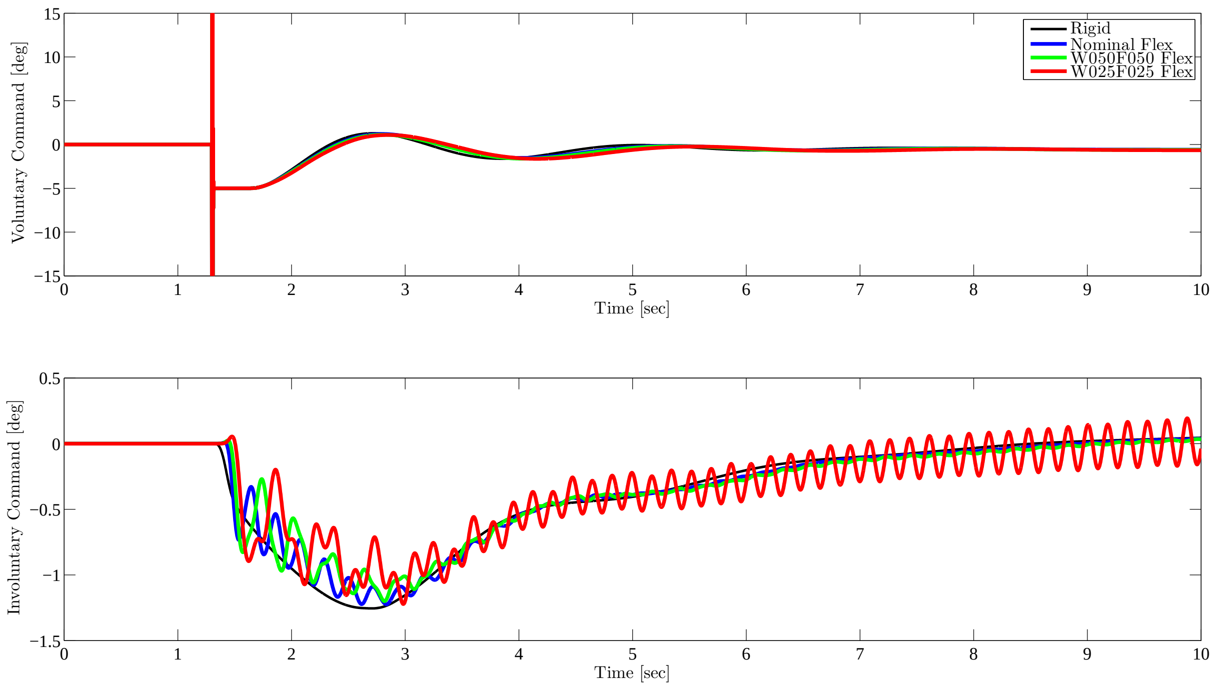

Figure 6: Pilot commands for the sitting erect position.

Figures 7 and 8 show the results for the gross acquisition capture task for the standing erect position. It can be seen that a more dampened aircraft response is obtained when compared to the standing erect position. Also, it is observed a smaller amplitude in the high frequency oscillation corresponding to the PAO.

As the biodynamic feedthrough transfer function for the standing erect case presents a much smaller magnitude, when compared to the two sitting cases, it is reasonable that the consequence of the inclusion of the biodynamic feedthrough effect for this case are attenuated.

3.2 Inceptor dynamics effects

In the first simulation of this section, the natural frequency of the sidestick is set to ω_n = 10 rad/s and damping ratio is set to ξ = 0.1. The results are shown in Figs. 9 and 10.

Comparing these results with Figs. 3 and 4, which depict the same scenario but neglecting the feel-system dynamics, it can be concluded that the inclusion of the inceptor dynamics affects the closed-loop oscillation characteristics. The first interesting result is the frequency of the oscillation for the W025F025 configuration, as it is now much smaller (around 14 rad/s for this aircraft) and corresponds to the first fuselage wing bending mode. It happens that the inceptor has a peak magnitude close to its natural frequency, potentializing the aircraft's response (including the elastic modes) close to this frequency.

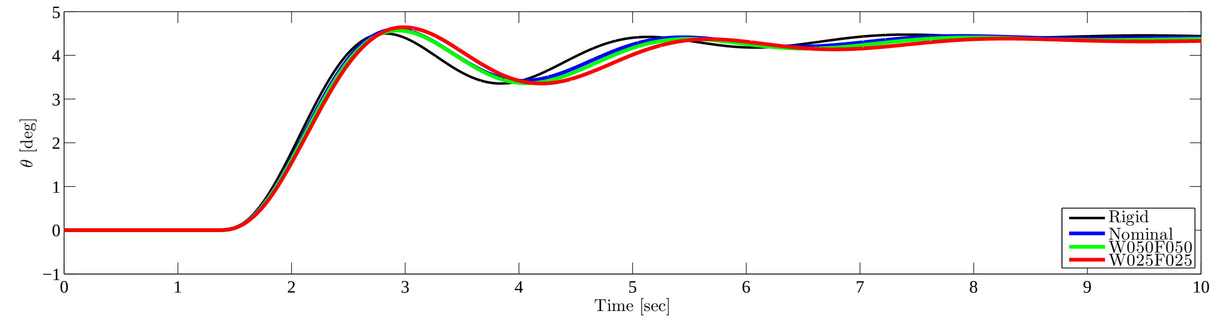

Figure 7: Pitch capture simulation for the standing erect position.

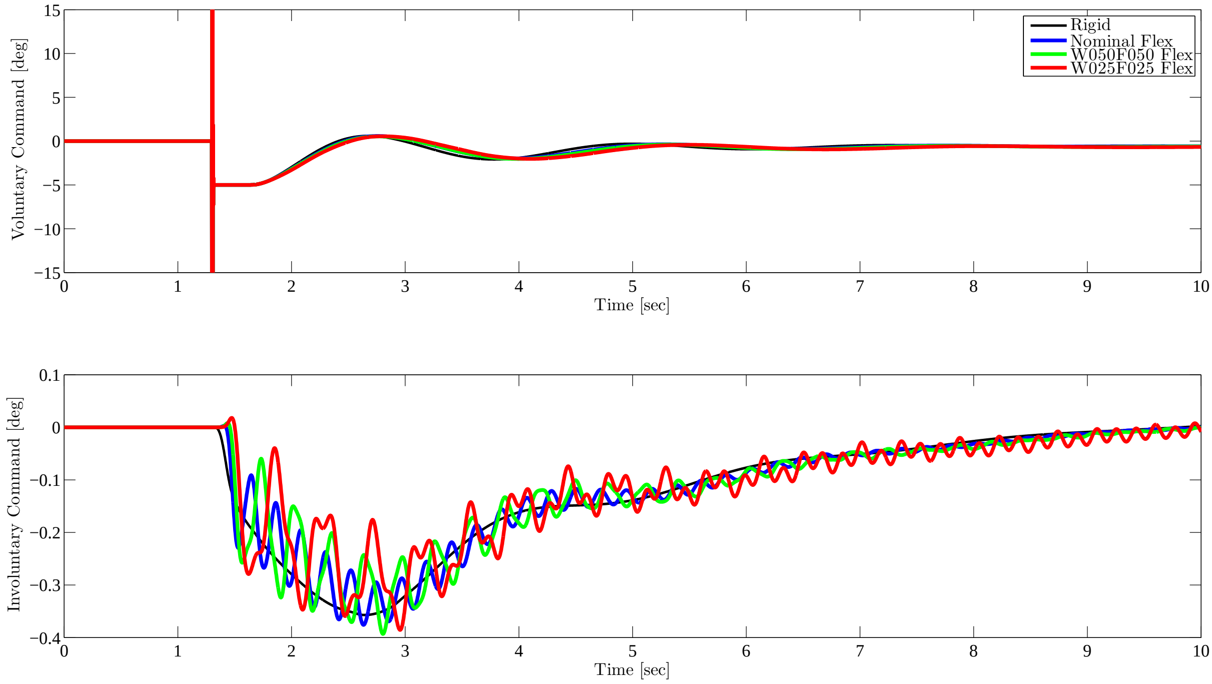

Figure 8: Pilot commands for the standing erect position.

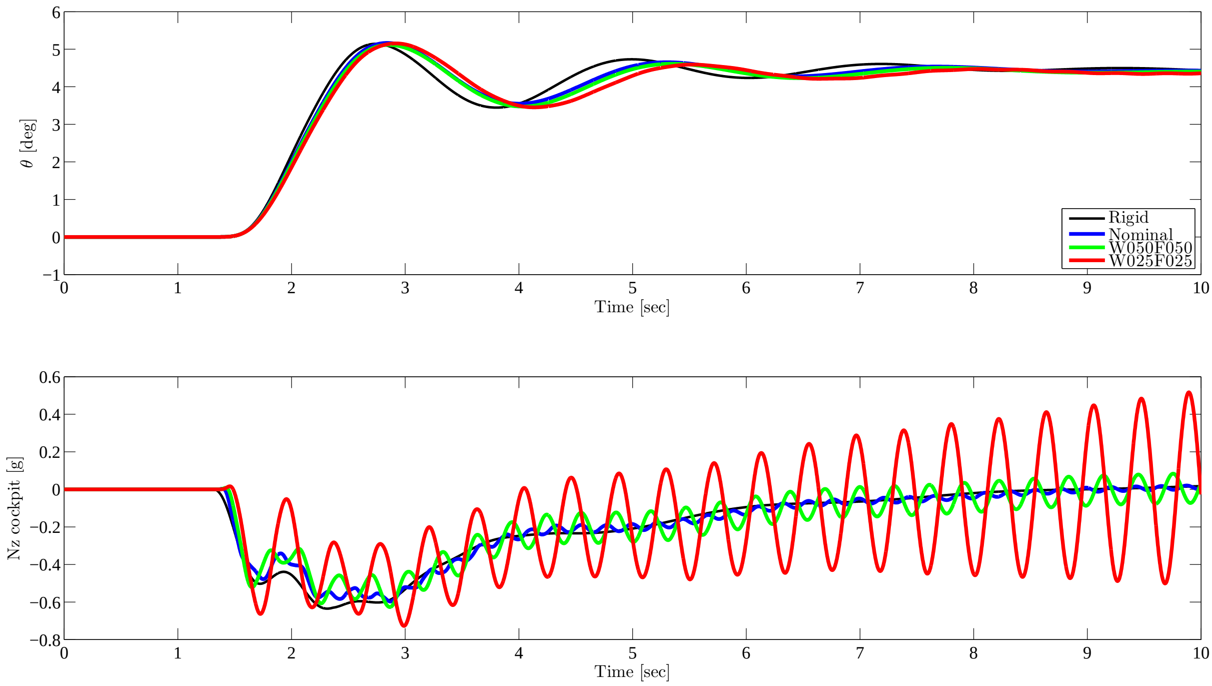

Figure 9: Pitch capture simulation for low frequency, poor-dampened stick.

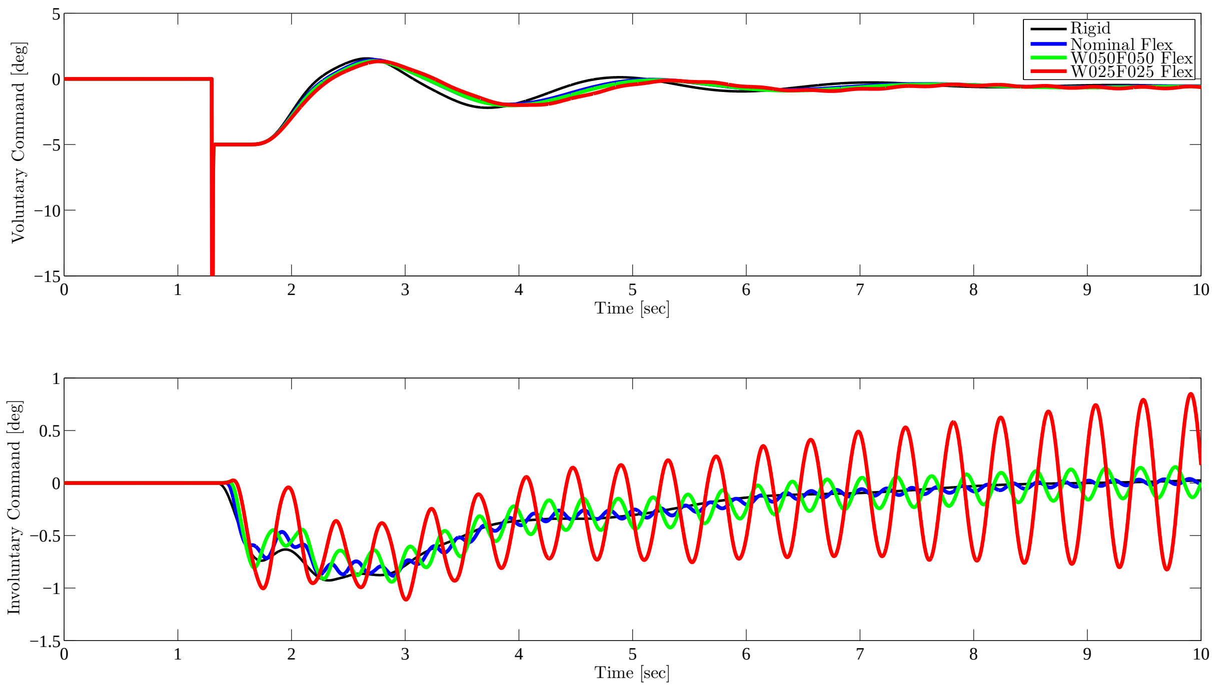

Figure 10: Pilot commands for the low frequency, poor-dampened stick.

If the feel-system damping ratio is increased to $\xi = 0.9$, the gross acquisition pitch capture simulation can be repeated, with the results shown in Figs. 11 and 12. As the increase of damping indeed reduces the magnitude of the frequency response of a second order dynamics system, the result is that the high frequency oscillations are now attenuated, while in the previous case they were unstable.

However, the pitch attitude signal measured at the CG now presents a capture task with less precision, with higher overshoot and a low dampened and low frequency oscillation. In other words, the increase in the damping ratio can minimize PAO severity, but can also increase the susceptibility of the aircraft to the PIO phenomenon.

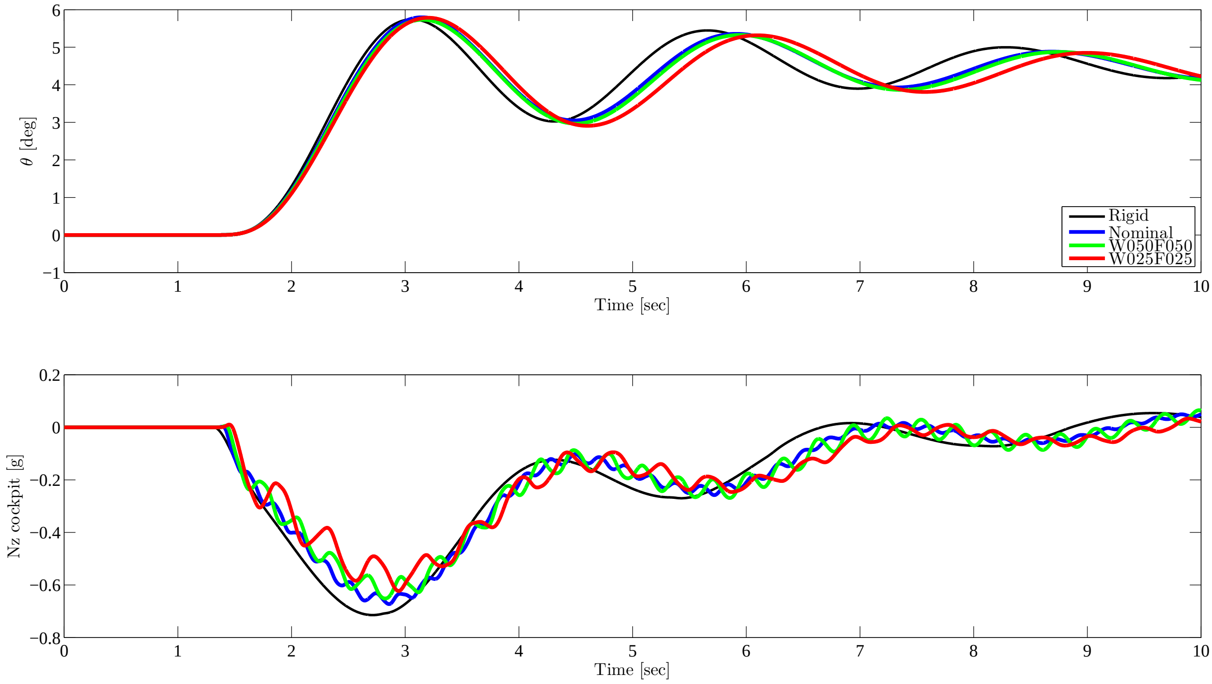

Figure 11: Pitch capture simulation for low frequency, well-dampened stick.

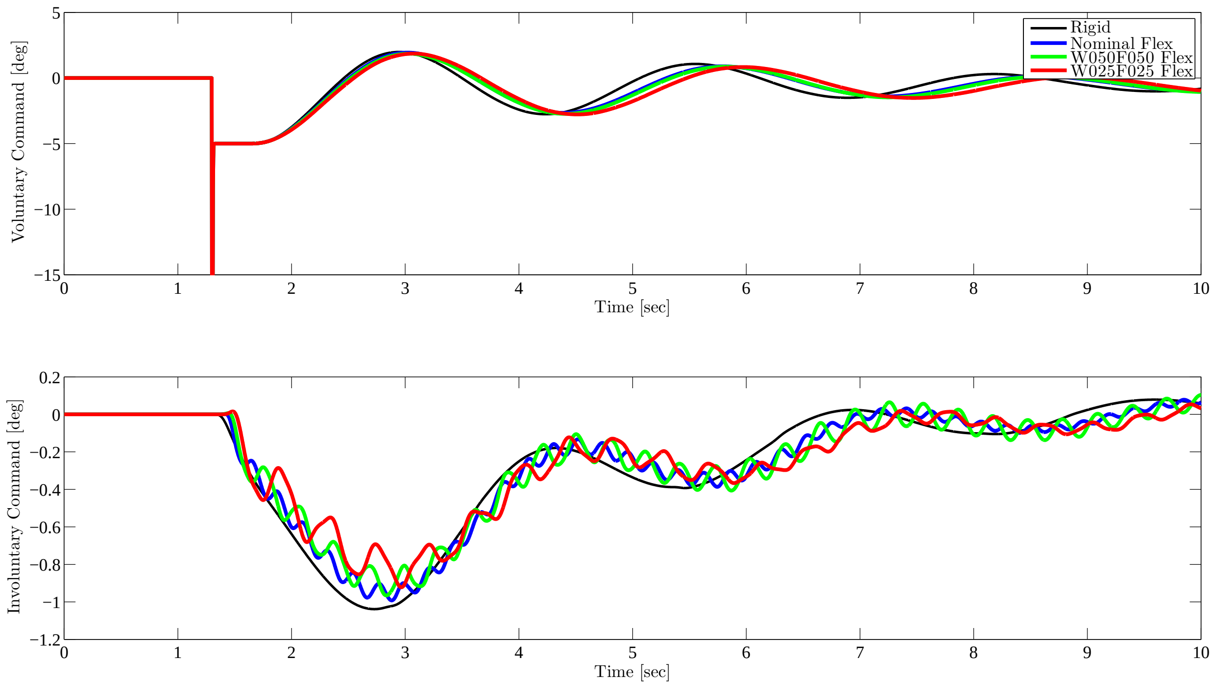

Figure 12: Pilot commands for the low frequency, well-dampened stick.

Natural frequency of the sidestick is now set to ω_n = 20 rad/s and damping is ξ = 0.1. Figures 13 and 14 depict the results of the simulation. The most affected aircraft is W050F050, since it has the natural frequency of the elastic mode corresponding to the first fuselage vertical bending (around 20.5 rad/s for this aircraft) closer to the natural frequency of the sidestick. As damping is low, oscillation increases and is divergent. Nominal flexibility also presents oscillation, but at a limit-cycle and at a smaller amplitude. W025F025 flexibility aircraft also presents a high-frequency oscillation due to the biodynamic feedthrough, but it is of much smaller amplitude. W050F050 aircraft also presents a PIO.

Nevertheless, it shall be mentioned that load factor at the cockpit reached peak values of almost 6g in this simulation, which is far beyond the structural limit of a transport class aircraft like the GNBA, which means that this PAO, if observed in practice, could lead to a potentially catastrophic scenario.

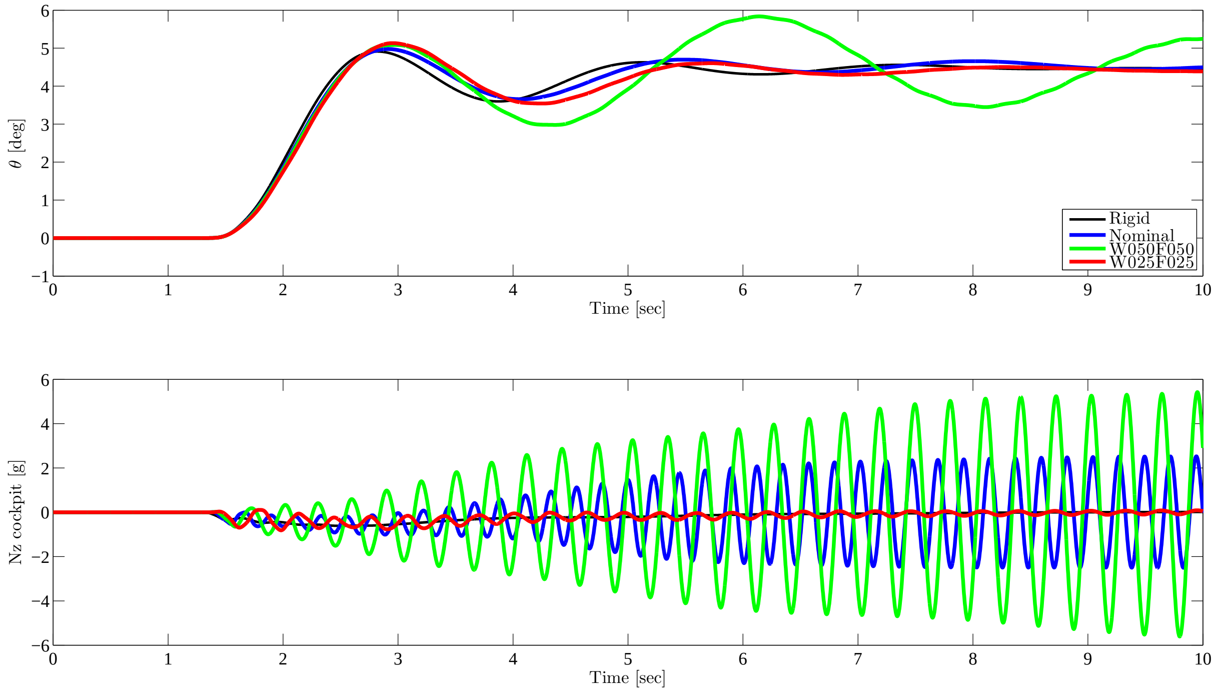

Figure 13: Pitch capture simulation for high frequency, poor-dampened stick.

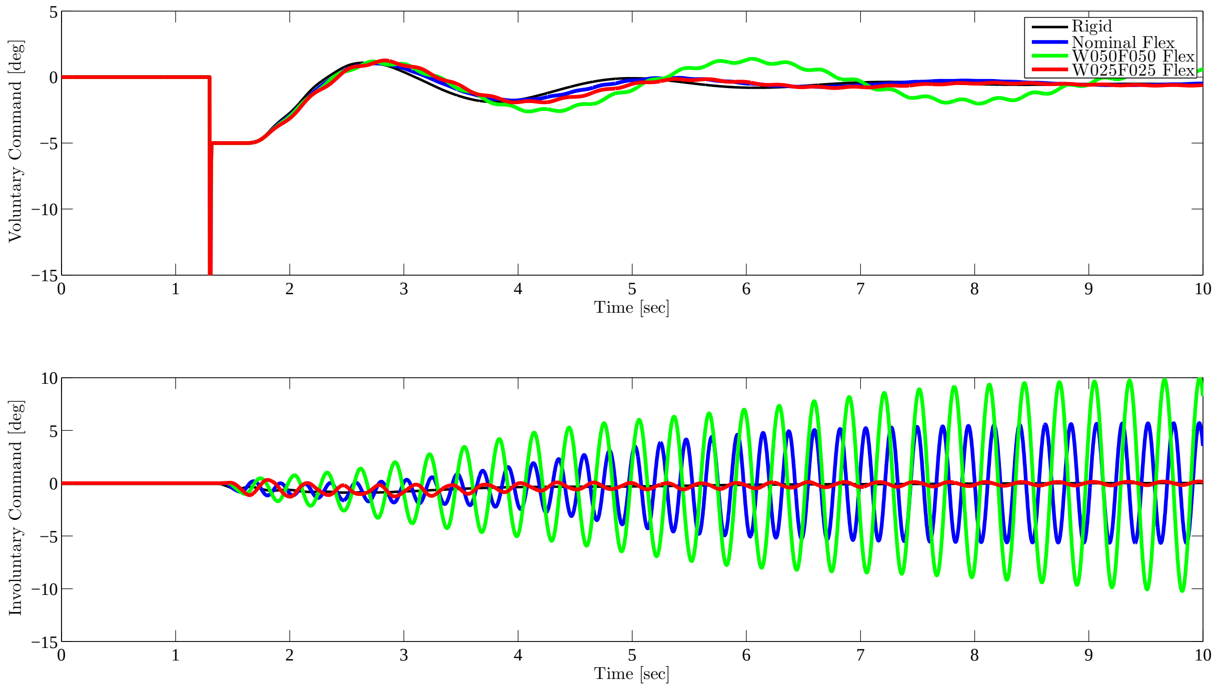

Figure 14: Pilot commands for the high frequency, poor-dampened stick.

The increase in sidestick damping to ξ = 0.9 leads to the results presented in Figs. 15 and 16. The oscillations are now still divergent, but at a much smaller magnitude. The cost to be paid is the reduction in the precision of the maneuver. Still, this PAO will not lead to a catastrophic event anymore.

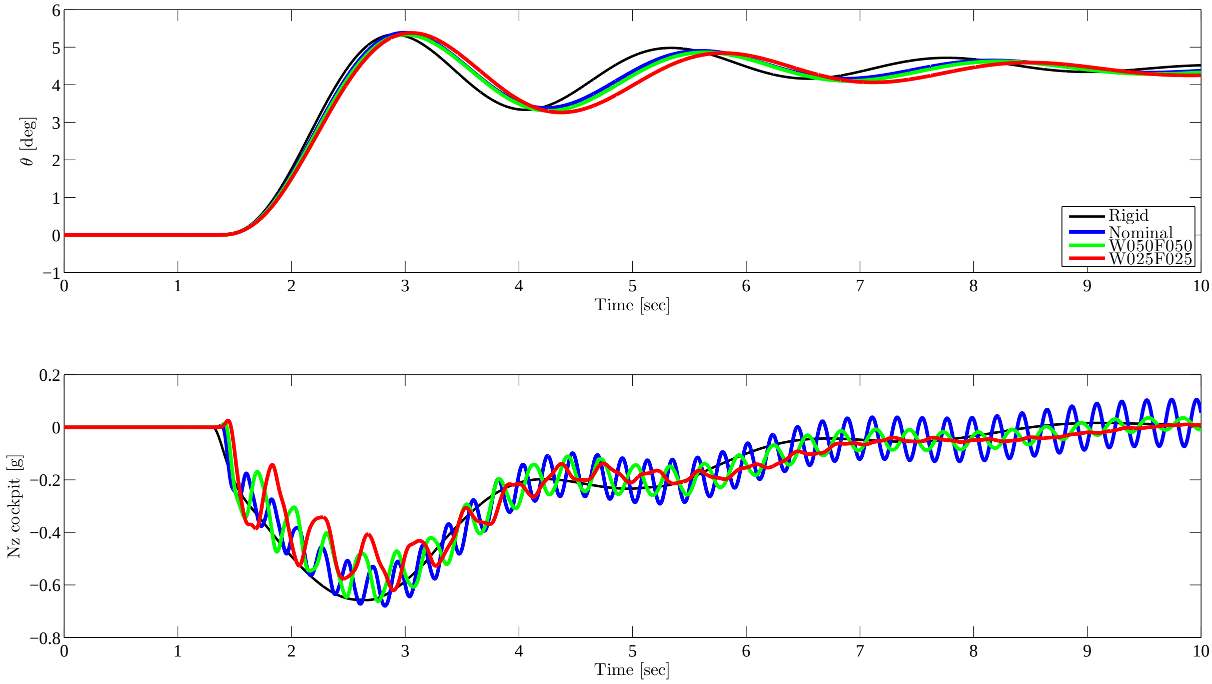

Figure 15: Pitch capture simulation for high frequency, well-dampened stick.

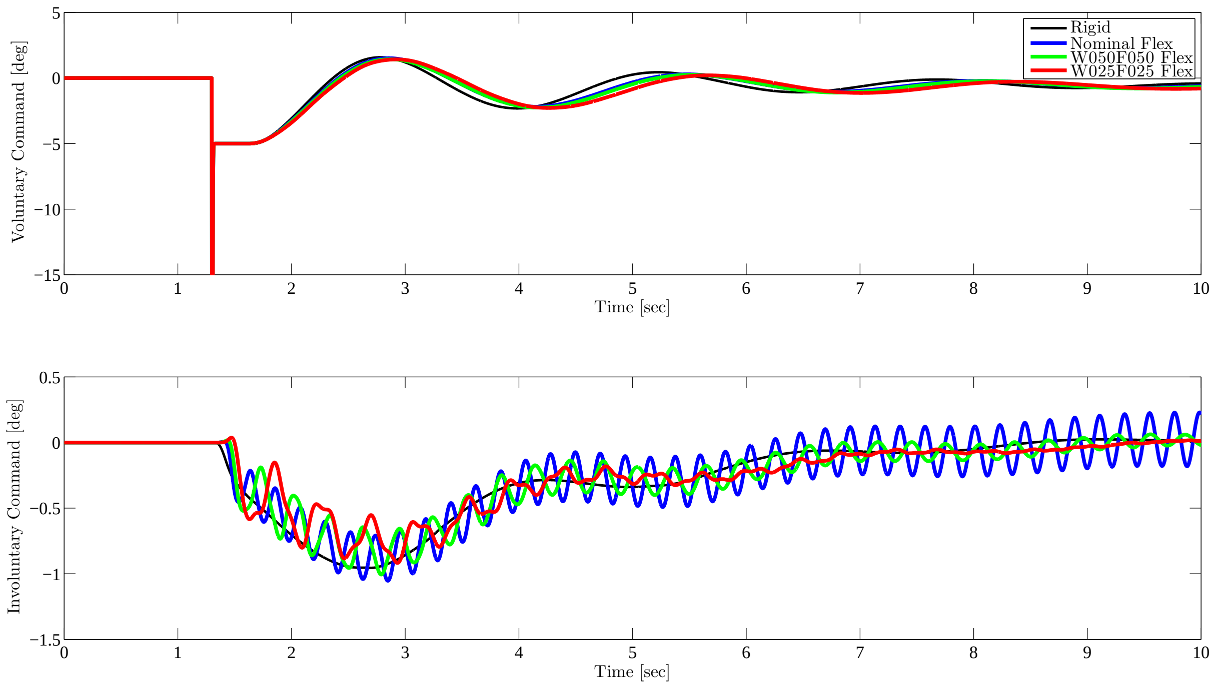

Figure 16: Pilot commands for the high frequency, well-dampened stick.

4 CONCLUSIONS

This paper presented several simulations considering variations on the biodynamic feedthrough model and the feel-system parameters of natural frequency and damping and their impact in aircraft's susceptibility to the Pilot-Augmented Oscillations (PAO) problem.

Simulations showed that variations in the biodynamic feedthrough model transfer function, such as the low frequency gain and both the frequency and the magnitude of the resonant peak, may affect the characteristics of the closed-loop response and therefore change the aircraft's PAO-proneness.

The feel-system dynamics plays a very important role in the development of PAO due to the biodynamic feedthrough effect, as natural frequency of the inceptor system may couple with some of the flexible modes of the aircraft. By changing the natural frequency of the inceptor, it's possible to change the exposition to the problem. However, if this frequency matches with one elastic mode that contributes to generate vibration on the cockpit, PAO occurs. Increasing sidestick natural frequency can be useful to minimize the magnitude of these oscillations, but this measure alone is not enough to eliminate the problem. Still, as the range of the natural frequencies of the elastic modes (due to variations on both mass distribution and flight condition) that cause PAO can be estimated in the early design phases of aircraft design, it can be an input to be considered into the definitions of the control inceptors system.

The other important parameter of the feel-system is the damping. PAO problem can be strongly minimized by increasing the value of damping. However, increasing damping has a collateral effect of increasing delays in the flight control system as well. And excessive delay may lead to PIO. In such scenario, a PAO problem is replaced by a PIO problem. Another possible solution for mitigating PAO, not explored in this paper though, is the development of notch filters. However, this solution can also lead to the same problem of increase in delays, replacing the PAO problem by a PIO one.

One relevant remark is that handling qualities criteria focused on the PIO problem usually adopt simplifications regarding the feel-system dynamics, often considering a fixed value for the inceptor dynamics. This idea basically relies on the assumption that the feel-system would only add some fixed delay to the final aircraft response. This premise is correct if the biodynamic feedthrough effect can be neglected. However, as the presented results show, this effect becomes more evident for more flexible aircraft and can lead to the occurrences of PAO. Up to date, there are no handling qualities criteria that deal with the PAO problem.

As a final result, the analysis herein presented, considering a mixed pilot model which comprises both the voluntary and the involuntary pilot models, including also the inceptors dynamics, was shown to be a promisory approach in the flight dynamics analysis for the design of more efficient control laws for more elastic aircraft.

5 REFERENCES

[1] Walden, R. B. *A Retrospective Survey of Pilot-Structural Coupling Instabilities in Naval Rotorcraft*, American Helicopter Society 63rd Annual Forum, 2007.

[2] Muscarello, V., Quaranta, G., Masarati, P. *Prediction and Simulator Verification of Roll Lateral Adverse Aeroservoelastic Rotorcraft-Pilot Couplings*, AIAA Journal of Guidance, Control and Dynamics, 2016, Vol.39: 42-60. doi: 10.2514/1.G001121.

[3] Allen, R., *Manual control performance and dynamic response vibration*, Systems Technology Incorporated, 1973.

[4] Lee, B. P., Vining, K. A., *Transport Aircraft Certification Testing for Pilot Closed Loop Dynamic Instability*, AIAA Atmospheric Flight Mechanics Conference, AIAA AVIATION Forum, AIAA-2018-4171. doi: 10.2514/6.2018-4171.

[5] Drewiacki, D, Silvestre, F. J. and Guimarães Neto, A. B. *Influence of airframe flexibility on pilot-induced oscillations*, AIAA Journal of Guidance, Control and Dynamics, 2019, doi: 10.2514/1.G004024.

[6] Venrooij, J., Mulder, M., van Paassen, M. M., Abbink, D. A., van der Helm, F. C. T., Blthoff, H. H. *How Effective is an Armrest in Mitigating Biodynamic Feedthrough*, 2012 IEEE International Conference on Systems, Man and Cybernetics, 2012.

[7] McRuer, Duane T., *Pilot Induced Oscillations - Human Dynamic Behavior*, NASA Contractor Report, 1995.

[8] Guimarães Neto, Antônio B. , *Flight dynamics of flexible aircraft using general body axes: a theoretical and computational study*,Thesis of Doctor in Science in Flight Mechanics - Instituto Tecnológico de Aeronáutica, São José dos Campos SP, 2014.

[9] Albano, E., Rodden, W. P., *A doublet-lattice method for calculating lift distributions on oscillating surfaces in subsonic flows*, AIAA Journal, v.7, n.2 p.279-285, 1968. doi: 10.2514/6.1968-73

[10] Eversman, W., Tewari, A., *Consistent rational function approximation for unsteady aerodynamics*, Journal of Aircraft, 1991, Vol.28: 545-552. doi: 10.2514/3.46062

[11] Waszak, Martin R., and Schmidt, David K., *Flight Dynamics of Aeroelastic Vehicles*, Journal of Aircraft, 1988.25:563-571.

[12] Coermann, R. R., *The mechanical impedance of the human body in sitting and standing position in low frequencies*, USAF Technical Report ASD-TR-61-492, 1961.

[13] AC 25-7C, *Flight Test Guide For Certification Of Transport Category Airplanes*, Federal Aviation Administration, 2012.

COPYRIGHT STATEMENT